



UNIVERSITY OF LEEDS

This is a repository copy of *Natural Biomaterial-Based Edible and pH-Sensitive Films Combined with Electrochemical Writing for Intelligent Food Packaging*.

White Rose Research Online URL for this paper:
<http://eprints.whiterose.ac.uk/147748/>

Version: Accepted Version

Article:

Zhai, X, Li, Z, Zhang, J et al. (9 more authors) (2018) Natural Biomaterial-Based Edible and pH-Sensitive Films Combined with Electrochemical Writing for Intelligent Food Packaging. *Journal of Agricultural and Food Chemistry*, 66 (48). pp. 12836-12846. ISSN 0021-8561

<https://doi.org/10.1021/acs.jafc.8b04932>

© 2018 American Chemical Society. This is an author produced version of a paper published in *Journal of Agricultural and Food Chemistry*. Uploaded in accordance with the publisher's self-archiving policy.

Reuse

Items deposited in White Rose Research Online are protected by copyright, with all rights reserved unless indicated otherwise. They may be downloaded and/or printed for private study, or other acts as permitted by national copyright laws. The publisher or other rights holders may allow further reproduction and re-use of the full text version. This is indicated by the licence information on the White Rose Research Online record for the item.

Takedown

If you consider content in White Rose Research Online to be in breach of UK law, please notify us by emailing eprints@whiterose.ac.uk including the URL of the record and the reason for the withdrawal request.



eprints@whiterose.ac.uk
<https://eprints.whiterose.ac.uk/>

1 Natural biomaterial-based edible and pH-sensitive films combined with
2 electrochemical writing for intelligent food packaging

3 Xiaodong Zhai^{†,1}, Zihua Li^{†,1}, Junjun Zhang^{†,1}, Jiyong Shi^{†,1}, Xiaobo Zou^{*,†,1}, Xiaowei
4 Huang^{†,1}, Yue Sun^{†,1}, Wen Zhang^{†,1}, Zhikun Yang^{†,1}, Mel Holmes^{‡,1}, Yunyun Gong^{‡,1},
5 Povey, Megan J^{‡,1}

6 [†]Agricultural Product Processing and Storage Lab, School of Food and Biological
7 Engineering, Jiangsu University, Zhenjiang, Jiangsu 212013, China

8 [‡]School of Food Science and Nutrition, the University of Leeds, Leeds LS2 9JT,
9 United Kingdom

10 ¹China-UK joint laboratory for nondestructive detection of agro-products, Jiangsu
11 University, Zhenjiang, Jiangsu 212013, China

12 * Corresponding author. Tel.: +86 511 88780174; fax: +86 511 88780201; Email:
13 zou_xiaobo@ujs.edu.cn

14 **ABSTRACT**

15 An edible and pH-sensitive film combined with electrochemical writing was developed
16 using gelatin, gellan gum and red radish anthocyanin extract for intelligent food packaging
17 applications. The composite film displays orange red-to-yellow color change over the pH
18 range 2-12. The tensile strength, ductility, and barrier response of the films to UV light and
19 oxygen improved with the increase of red radish anthocyanin concentration. Multicolor
20 patterns were successfully drawn on the film using an electrochemical writing method. The
21 composite films acted as gas sensors which presented visible color changes in the presence
22 of milk and fish spoilage, while the written patterns were well preserved. Accordingly, this
23 composite film with written patterns could be an easy-to-use indicator with great potential
24 for monitoring food spoilage as part of an intelligent packaging system.

25 **KEYWORDS: intelligent food packaging; gelatin; gellan gum; red radish**
26 **anthocyanins; electrochemical writing; film**

27 **1. INTRODUCTION**

28 Intelligent food packaging has received great interests in the last decades, because of
29 their potential for monitoring the condition of packaged foods or the surrounding
30 environment.¹ Generally, intelligent food packaging systems can be realized by three main
31 technologies, namely sensors, indicators and data carriers.² Among these systems,
32 indicators (e.g. freshness indicators, time-temperature indicators and gas indicators) which
33 could provide qualitative or semi-quantitative information by means of a color change have
34 been widely studied since they are easy to fabricate and can be read by naked eye.

35 In recent years, many pH-sensitive indicators have been developed to monitor food
36 quality. This was because various non-neutral volatile gases, such as amines, hydrogen
37 sulfide and carbon dioxide, can be generated from foods during spoilage. When these
38 volatile gases diffused to the headspace of the packages, they could react with the pH-
39 sensitive indicators and thus make color changes of the indicators. Generally, the pH-
40 sensitive materials were composed of pH dyes and a solid matrix to immobilize the pH
41 dyes.^{3, 4} Considering that traditional synthetic pH dyes with potential harmful effects to
42 human beings are not ideal for food packaging,⁵ more attentions have recently been paid
43 to natural and safe pigments, such as anthocyanins⁶⁻¹⁴ and curcumin.¹⁵⁻¹⁸ In addition, due
44 to the public concern over environmental problems caused by plastics, there is a greater
45 demand for packaging materials made by eco-friendly biopolymers with good film-
46 forming properties, such as starch, chitosan, gums, alginate, agar, gelatin and so forth.

47 Red radish (*Raphanus sativus* L.) (RR) is a anthocyanins-rich vegetable,¹⁹ in which
48 anthocyanins mainly exist at acylated structures.²⁰ Anthocyanins extracted from red radish

49 are widely used as natural food-coloring agents because of their high stability and their
50 orange-red color similar to that of synthetic Food Red No. 40.^{20, 21} As red radish is also
51 widespread and low cost, the red radish anthocyanins (RRA) could be a good resource of
52 pH-sensitive pigments. The solid matrix used to immobilize anthocyanins is also of great
53 importance. Gelatin is a denatured protein from the triple helix of collagen. It is accepted
54 as “Generally Recognized as Safe” (GRAS) substance in the area of food additives by the
55 US Food and Drug Administration (FDA).²² Gelatin is also considered as a promising
56 natural polymer for packaging applications because of its renewability, biodegradability
57 and film-forming property.²³ Particularly, gelatin films possess good oxygen barrier
58 property.²² This may be used to protect packaged foods from being oxidized to some extent
59 and thus improve their shelf life. However, poor mechanical properties (such as frangibility)
60 have been described as one of the disadvantages of gelatin films.²⁴ To compensate this
61 shortcoming, gelatin is generally cross-linked and/or combined with other polymers, such
62 as sodium alginate²⁵ and chitosan.²⁶ Gellan gum, a linear negatively charged
63 exopolysaccharide, is biodegradable and non-toxic in nature. Four repeating carbohydrates
64 are present in the main chain of gellan gum, which includes two d-glucose carbohydrates,
65 one L-rhamnose, and one D-glucuronic acid.²⁷ It has received both US FDA and EU (E418)
66 approval for application mainly as a multi-functional gelling, stabilizing and suspending
67 agent in a variety of foods and personal care products.²⁸ Importantly, it was found that the
68 mechanical properties of gelatin film could be significantly improved by gellan gum.²⁹
69 Furthermore, a recent study showed that gellan gum could enhance the thermal stability of
70 anthocyanins.³⁰ Hence, the gelatin/gellan gum blend could be a good film-forming agent
71 to immobilize anthocyanins.

72 Most food packaging materials are printed in order to provide information about the
73 packaged foods and many inks are still mainly derived from petrochemical feedstock,
74 which brings significant environment and sustainability problems to modern society.³¹ In
75 addition, the migration of unsafe printing inks from packaging to food can be a risk for
76 consumers health.³² To solve these problems, new inks such as edible inks and new
77 techniques for printing are very desirable.³³ Recently, Wu, et al. ³⁴ successfully printed on
78 polysaccharide film by an electrochemical method based on the pH response color change
79 of anthocyanins. As anthocyanins are safe and biodegradable, this electrochemical writing
80 can be regarded as a green printing method. However, the related work of electrochemical
81 writing on edible films is still limited.

82 In this study, we aimed to develop a new pH-sensitive and edible film by using RRA as
83 the pH-sensitive pigment and gelatin/gellan gum blend as the film-forming agent,
84 respectively. The fundamental properties of films, such as microstructure, mechanical
85 properties and gas permeability properties were first investigated. Then, multicolor patterns
86 were written on this polysaccharide/protein composite film by using an electrochemical
87 writing method. Finally, the film combined with written patterns was used to indicate milk
88 and fish quality.

89 **2. MATERIALS AND METHODS**

90 **2.1. Materials and Reagents.** Fresh red radish (cultivar ‘Xinlimei’) and live black carp
91 were purchased from local market, and pasteurized milk was bought from a local cattle
92 farm (Zhenjiang, China). Gelatin (type B, pig skin) was purchased from Sigma-Aldrich Inc.
93 (St. Louis, MO, USA). Low-acyl gellan gum was bought from Dancheng Caixin sugar

94 industry Co., Ltd. (Dancheng, China). Other chemical agents, such as ethyl alcohol, calcium
95 chloride, acetic acid, ammonium hydroxide, acetonitrile and formic acid were bought from
96 Sinopharm Chemical Reagent Co., Ltd (Shanghai, China).

97 **2.2. Extraction of anthocyanins from red radish.** Fresh red radishes were peeled, cut
98 into pieces and dried at 65 °C under vacuum. Then, the dried red radishes were crushed
99 into powder and transferred to 80% ethanol aqueous solution with a solid-liquid ratio of
100 1:10. After stirring at 35 °C for 6 h, supernatant of the solution was collected through
101 filtration using a 25- μ m filter paper. Ethanol in the supernatant was removed with a vacuum
102 rotary evaporator at 45 °C in dark. Finally, the concentrated RRA extract solution was
103 freeze-dried under vacuum and the obtained RRA extract powder was stored at 4 °C in a
104 brown bottle filled with nitrogen.

105 The anthocyanins content in lyophilized RRA extract powder was measured by the pH
106 differential method.³⁵ Absorbance of sample at 520 and 700 nm was measured using a UV-
107 Vis spectrophotometry (Agilent CARY 100, Varian Corporation, USA). The anthocyanin
108 content was expressed in mg/g.

109 **2.3. Preparation of films.** Firstly, 100 mL aqueous dispersion containing 3 g of gelatin
110 (G) and 1 g of gellan gum (GG) was heated at 85 °C in a water bath and stirred with a
111 magnetic stirrer for 0.5 h to form a clear solution. Under this constant temperature, 30 mg
112 of CaCl₂·2H₂O was added into the solution with continuous stirring. Based on the
113 calculated anthocyanins content (303.42 ± 7.82 mg/g) (refer to section 2.3), RRA extract
114 powder was then added to the solution to obtain an anthocyanin contents of 5 mg/100 mL,
115 10 mg/100 mL, 15 mg/100 mL and 20 mg/100 mL, expressed as RRA5, RRA10, RRA15

116 and RRA20. A control solution containing gelatin, gellan gum and $\text{CaCl}_2 \cdot 2\text{H}_2\text{O}$ was also
117 prepared. After degassing with a sonicator at $85\text{ }^\circ\text{C}$, 12 g of the film-forming solution was
118 immediately poured into a clean and smooth plastic Petri dish with a 9 cm diameter. Then,
119 firm hydrogels were formed after the solutions were cooled down. The hydrogels were
120 dried to films by putting the Petri dishes on a horizontal platform in an oven at $45\text{ }^\circ\text{C}$ for 2
121 h. After that, the film was peeled from the Petri dishes and stored in an incubator at $4\text{ }^\circ\text{C}$
122 with 75% RH for further use.

123 In order to prepare films with electrochemical writing, the above-mentioned hydrogels
124 containing RRA were firstly taken out from the Petri dish before drying. The hydrogel was
125 contacted with a platinum (Pt) plate connected to the cathode of an electrochemical
126 analyzer (CHI660E, CH Instruments Co., Shanghai, China). Then, a Pt needle (diameter
127 0.5 mm) connected to the anode of the electrochemical analyzer touched the upper surface
128 of the hydrogel. Under a constant current, hydrogen ions were produced around the
129 platinum needle and thus induced an orange red color of RRA. On the contrary, when the
130 Pt plate was connected to the anode of the electrochemical analyzer and the Pt needle was
131 connected to the cathode of the electrochemical analyzer, hydroxyl ions were produced
132 around the Pt needle and thus induced a green color of RRA. The movement of the platinum
133 needle was procedurally controlled by a mechanical arm with a step precision of $0.1\text{ }\mu\text{m}$
134 (DOBOT M1, Shenzhen Yuejiang Technology Co., Ltd, China). The hydrogel was
135 immediately dried in a vacuum-drying oven at $70\text{ }^\circ\text{C}$ to form a film and the film was stored
136 at $4\text{ }^\circ\text{C}$ with 75% RH before use.

137 **2.4. Characterization of the films**

138 **2.4.1. Color response to pH variation.** UV-vis spectra of films were measured using a
139 UV-vis spectrophotometer (Agilent CARY 100, Varian Corporation, USA). Firstly, pH
140 buffer solutions (pH 2-12) were prepared by using 0.2 M disodium hydrogen phosphate,
141 0.2 M citric acid and 0.2 M sodium hydroxide solutions with different proportions. Then,
142 films were cut into squares (1 cm × 1 cm) and immersed in the buffer solutions for 5 min.
143 The spectra of the films in the range of 400-800 nm were obtained using air as the blank.

144 **2.4.2. Microstructure observation.** The micrographs of the films were recorded by a
145 field emission scanning electron microscope (FE-SEM) (S-4800, Hitachi High
146 Technologies Corporation, Japan). The films were first freeze fractured by liquid nitrogen
147 before measurement. Samples were attached to double-sided adhesive tape and mounted
148 on the specimen holder, then sputtered and coated with gold under vacuum.

149 **2.4.3. Mechanical properties.** Tensile strength (TS) and elongation-at-break (EB) of the
150 films were measured with an Instron Universal Testing Machine (Model 4500, Instron
151 Corporation, Canton, MA, USA) using a modified ASTM D882-00 (ASTM, 2000b)
152 procedure. Samples were conditioned at 25 °C and 50 ± 3% RH in a desiccator containing
153 magnesium nitrate saturated solution for 2 d prior to analysis. Each film was cut in
154 rectangular strips with 60 mm length and 20 mm width. The initial grip separation and
155 crosshead speed were set at 40 mm and 0.6 mm/s respectively. The TS and EB were
156 calculated as the equation (1) and (2), respectively. Measurements represent an average of
157 six samples.

158
$$TS = F_{\max} / S \tag{1}$$

159 $E(\%) = 100 \times \Delta l / l_0$ (2)

160 where TS was the tensile strength (MPa); F_{\max} was the maximum load (N); S was the
161 initial cross-sectional area of the film sample (mm²); E was the elongation-at-break; Δl
162 was the extension of the film (mm) and l_0 was the initial test length of the film (40 mm).

163 **2.4.4. Transparency measurement.** The optical transmittance of GGG and GGG-RRA
164 films (2 cm × 1 cm) were measured in the range of 200–800 nm with air as the blank by
165 using the UV–vis spectrophotometer.

166 **2.4.5. Water vapor permeability.** Water vapor permeability (WVP) of films was
167 determined gravimetrically using a standard test method (ASTM E96-05). The film
168 samples that had previously equilibrated at 50% RH for 48 h were sealed on glass cups
169 containing dried silica gel (0% RH). The cups were then placed in desiccators containing
170 saturated Mg(NO₃)₂ solution (50% RH) at 25 °C. The cups were weighed at 1-h interval
171 until a steady state was reached. The water vapor transmission rate (WVTR) of a film was
172 determined from the slope of the regression analysis of weight gain of moisture (Δm) that
173 transferred through a film area (A) during a definite time (t), as shown in equation (3). Then,
174 the WVP of the film was calculated based on the WVTR, as shown in equation (4).
175 Measurements represent an average of six samples.

176 $WVTR = \Delta m / (A \times t)$ (3)

177 $WVP = WVTR \times x / \Delta P$ (4)

178 where Δm is the weight gain of the cup (g); x is the film thickness (m); A is the exposed
179 area (m^2); ΔP is the partial water vapor pressure difference across the film (1583.7 Pa at
180 25°C); t is the time (h).

181 **2.4.6. Oxygen permeability.** Oxygen permeability (OP) of the film was estimated at
182 25°C and 50% RH with an automated oxygen permeability testing machine (GTR-7001,
183 SYSTESTER, China) following the standard method (ASTM D3985-05, 2005). Film was
184 placed on a stainless-steel mask with an open testing area of 48 cm^2 . Oxygen and nitrogen
185 were respectively flowed on each side of the films. Oxygen transmission rate (OTR) was
186 measured and OP was calculated according to equation (5). Measurements represent an
187 average of six samples.

$$188 \quad \text{OP} = \text{OTR} \times x / \Delta P \quad (5)$$

189 where OTR is the oxygen transmission rate ($\text{cm}^3 \cdot \text{m}^{-2} \cdot \text{d}^{-1}$); x is the film thickness (m); ΔP is
190 the partial pressure of oxygen (1.013×10^5 Pa at 25°C).

191 **2.4.7. Color stability.** The colorimetric films were stored in incubators at 4°C and 25°C
192 with 75% RH under fluorescent lights. The images of the colorimetric films were captured
193 every day for two weeks by an optical scanner (Scanjet G4050, HP) and analyzed by a user
194 program in Matlab R2012a (Matworks Inc., Natick, MA, USA). The stability of the
195 colorimetric films was defined as the relative colour change, according to our previous
196 study:³⁶

$$197 \quad \Delta R = |R_0 - R_1| \quad (6)$$

198 $\Delta G = |G_0 - G_1|$ (7)

199 $\Delta B = |B_0 - B_1|$ (8)

200 $S = (\Delta R + \Delta G + \Delta B) / (R_0 + G_0 + B_0) \times 100\%$ (9)

201 where R_0 , G_0 , B_0 were the initial gray values of the red, green and blue, R_1 , G_1 , B_1 were the
202 gray values of the red, green and blue after storage. S was the relative color change of R ,
203 G and B values.

204 **2.4.8. Color response to basic and acid gases.** Response of the colorimetric films
205 toward volatile ammonia in term of their color changes was performed using absorbance
206 measurements. The colorimetric films were hang up in an Erlenmeyer flask (500 mL) at 1
207 cm above the ammonia solution (80 mL, 8 mM) at 25°C.

208 **2.5. Application of films in monitoring food quality**

209 **2.5.1. Milk spoilage trial.** 20 mL of pasteurized fresh milk was poured into an unused
210 plastic Petri dish (diameter 90 mm) with a lid. In the middle of the lid, a square hole was
211 cut using a knife. Then the film was fixed on the lid to cover the hole. The Petri dish was
212 sealed with Vaseline and placed in an incubator at 25 °C with 75% RH. During milk
213 spoilage, volatile gases were generated from the milk and diffuse through the film, making
214 a color change of the film. The images of the film were captured using the optical scanner.
215 The acidity of milk was measured by acid-base titration method according to a previous
216 literature.³⁷

217 **2.5.2. Fish spoilage trial.** Fresh black carp (*Mylopharyngodon piceus*) was cut into
218 strips after removing its innards, head, tail and scales. Like the milk spoilage trail, 25 g of
219 black carp was put into the plastic Petri dish and the film was fixed on the lid to cover the
220 hole. The Petri dish was placed in an incubator at 4 °C with 75% RH. The total volatile
221 basic nitrogen (TVB-N) content was measured according to a previous literature.³⁸

222 **3. RESULTS AND DISCUSSION**

223 **3.1. Color and UV-vis spectra of RRA and GGG-RRA film.** In this study, RRA was
224 used as the pH-sensitive pigment to develop packaging films, so the color response of RRA
225 and GGG-RRA film to pH variation was firstly investigated. Fig. 1A shows that RRA
226 solutions changed from orange red to yellow when pH increased from 2 to 12. In detail,
227 RRA solution turned from deep orange red to light orange over the pH range of 2-7. At
228 weak basic conditions, the color became purple (pH 8-9). Then, the color changed to yellow
229 green (pH 10) and finally to yellow (pH 10-12). Corresponding to color changes in RRA
230 solutions, the maximum absorption peak presented red-shifts. As shown in Fig. 1B, the
231 maximum absorption peak obtained at pH 2 was around 510 nm, which gradually shifted
232 to 520 nm when the pH increased to 6. Meanwhile, the maximum absorption values
233 decreased. As the pH increased over 7, the maximum absorption peak shifted to
234 approximately 580 nm. At the same time, the absorption values gradually increased when
235 pH increased from 7 to 10 and then decreased when pH increased from 10 to 12. The
236 absorbance ratio at 580 nm versus 510 nm (A_{580}/A_{510}) indicates the increase of green
237 intensity compared to red. The calibration curve (Fig. 1B inset) showed that values of
238 A_{580}/A_{510} in PSPE solution increased and then decreased over the range of pH 2-9. An
239 exponential calibration curve was established between the pH in the range of 2-9 and

240 A_{580}/A_{510} of the RRA solution, as formula (10), where x and y were the pH and A_{580}/A_{510} ,
241 respectively.

$$242 \quad y = 0.1399e^{0.2745x}, R^2 = 0.9823 \quad (10)$$

243 The GGG film containing RRA showed similar color (Fig. 1C) and spectra (Fig. 1D)
244 changes with RRA in response to pH variation. An exponential calibration curve was also
245 established between the pH in the range of 2-9 and A_{580}/A_{510} of the GGG-RRA film (Fig.
246 1D inset), according to the formula (11), where x and y were the pH and A_{580}/A_{510} ,
247 respectively.

$$248 \quad y = 0.2911e^{0.1583x}, R^2 = 0.9791 \quad (11)$$

249 Similar exponential calibration curves were also found in anthocyanins extracted from
250 purple sweet potato (PSP) and film containing PSP anthocyanins.³⁹ The exponential
251 calibration curve between pH and A_{580}/A_{510} for the GGG-RRA film indicated that RRA
252 maintained good chemical activity in the GGG film. The visible color changes of GGG-
253 RRA film toward pH change implied it was capable of indicating pH-related food quality.

254 **3.2. Microstructure of the films.** The SEM images showed that GGG film had a highly
255 compact and dense appearance of cross section (Fig. 2A). This indicated that gelatin and
256 gellan gum had excellent compatibility with each other due to the intermolecular
257 interaction. Similar homogeneous structure of composite G and GG film was also observed
258 in a previous study.⁴⁰ When a low content of RRA (i.e. 5 mg/100 mL) was added into the
259 GGG film, some small spindrift-like structures appeared and was uniformly distributed in
260 the film (Fig. 2B). With the increase of RRA content, the GGG-RRA films showed obvious

261 aggregation of spindrift-like structures and stratification (Fig. 2C and Fig. 2D). When a
262 relatively high content of RRA was added, the GGG-RRA20 film in turn became more
263 uniform than the GGG-RRA10 and GGG-RRA15 film even though the size of spindrift-
264 like structures was larger (Fig. 2E). This phenomenon could be explained by the gelation
265 process of both gelatin and gellan gum. During the gelation formation of gelatin, junction
266 zones were formed by small segments of two or three polypeptide chains reverting to the
267 collagen triple helix-like structure.⁴¹ It has been reported that the addition of phenolic
268 compounds promote the formation of hydrogen bonds among the three helices.⁴² For the
269 gellan gum, the formation of gels was closely affected by the pH of the solution. As gellan
270 gum is a linear anionic polysaccharide, the aggregation of gellan gum helices in water was
271 impeded by the intermolecular repulsion between negatively charged carboxylic groups on
272 the gellan gum, while this intermolecular repulsion can be weakened with the decrease of
273 pH of the solution, resulting in an enhancement of junction zone formation.⁴³ In this study,
274 RRA as a phenol compound could also contribute to the gelation of gelatin. At the same
275 time, with the increase of the RRA content, the pH of the solution decreased, contributing
276 the gelation of gellan gum. Therefore, more intermolecular cross-linking within gelatin
277 molecules and gellan gum molecules were generated, leading to partial phase separation of
278 gelatin and gellan gum. As shown in Fig. 2B-D, the continuous and compact phase with
279 parallel-arranged long chains could largely comprise gelatin molecules, while the coarse
280 phase could largely comprise gellan gum. However, when the RRA content was at a
281 relatively high level (20 mg/100 mL), the phase separation between gelatin and gellan gum
282 molecules in the GGG-RRA20 film was not as obvious as that in the GGG-RRA10 and

283 GGG-RRA15 films. This might be due to excessive RRA having a steric hindrance effect
284 on the formation of crosslinks among gelatin and gellan gum chains.

285 **3.3. Mechanical and barrier properties.** TS represents the capacity of the films to
286 withstand loads tending to elongate and EB expresses the capability of the films to resist
287 changes of shape without crack formation. The TS and EB of the GGG and GGG-RRA
288 films are shown in Fig. 3A. With the increase of RRA content, the TS and EB of the films
289 both become higher, indicating improved coupling strength and ductility of the films. The
290 changes in mechanical properties of the films could be explained by the intermolecular
291 interaction of G and GG in the absence and presence of RRA. The higher TS of the films
292 in the presence of RRA could be due to the enhanced cross-linking among G and GG chains,
293 respectively, as mentioned in section 2.3. Generally, an improved TS of a film was
294 accompanied by a sacrifice of EB. However, the EB of the GGG-RRA films also increased
295 with the increase of RRA. This could be due to the layer structure of the GGG-RRA films
296 that endowed them with better flexibility compared to the GGG film.

297 Fig. 3B shows the UV-vis transmission spectra and images (inset) of GGG and GGG-RRA
298 films. Pure GGG film was colorless and had a transparency of over 80% in the visible range
299 of 400-800 nm. The incorporation of RRA into GGG film resulted in an orange color which
300 became deeper with the increase of RRA content. The barrier property of the film to UV
301 light could be obtained from the spectra in the range of 200-400 nm. GGG film presented
302 excellent barrier properties to UV light in the range of 200-245 nm where the
303 corresponding transparencies were lower than 1%, similar to a previous gelatin film.⁴⁴
304 Moreover, the UV light barrier ability of the films were significantly enhanced with RRA,
305 since the films with higher RRA content showed improved barrier ability over broader

306 spectra ranges. GGG-RRA20 film presented strong barrier ability to UV light in the range
307 of 200-360 nm. These results could be due to the fact that RRA as a phenolic compound is
308 favorable for the adsorption of UV radiation.⁴⁵ The good UV light barrier properties of
309 GGG-RRA films may be beneficial for food preservation because UV light is known to
310 induce deleterious change, particularly lipid oxidation, in foods.⁴⁶

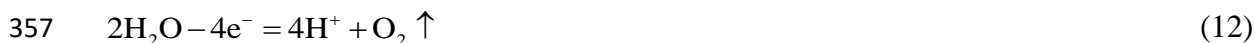
311 Fig. 3C shows the effect of RRA on the WVP of GGG films. Pure GGG film had a WVP
312 value of $2.83 \text{ g}\cdot\text{mm}\cdot\text{m}^{-2}\cdot\text{kPa}^{-1}\cdot\text{h}^{-1}$, which was several orders of magnitude higher than that
313 of polyethylene (PE) and poly(vinylidene chloride) (PVDC) films.⁴⁷ The high WVP of
314 GGG film could be due to the hydrophilic nature of gelatin and gellan gum. With the
315 increase of RRA content, the WVP of the films presented a first decline followed by a rise.
316 For GGG-RRA10 film, the WVP was $1.25 \text{ g}\cdot\text{mm}\cdot\text{m}^{-2}\cdot\text{kPa}^{-1}\cdot\text{h}^{-1}$, which was lower than a half
317 of the WVP value of the GGG film. As the RRA content increased to 20 mg/ 100 mL, the
318 GGG-RRA20 film showed a comparable WVP ($3.17 \text{ g}\cdot\text{mm}\cdot\text{m}^{-2}\cdot\text{kPa}^{-1}\cdot\text{h}^{-1}$) to the GGG film.
319 The permeability of a film largely depends on its chemical structure, morphology and
320 hydrophilicity, regardless of the environment conditions. The initial decrease of WVP of
321 films with the increase of RRA content to 10 mg/ 100 mL could be due to anthocyanin
322 enhancement of the interactions of both gelatin and gellan gum molecules, lowering the
323 amount of gelatin and gellan gum molecules needed to form hydrophilic bonding with
324 water and subsequently leading to a decrease in the affinity of the films towards water.
325 Meanwhile, anthocyanins as phenolic components could form mainly non-covalent
326 hydrophobic interactions with gelatin and gellan gum⁴⁸ and thus reduce the hydrophilicity
327 of the films. However, a significant increase of WVP of the film was observed from the
328 GGG-RRA15 and GGG-RRA20 films. This may be due to the high hydrophilicity of

329 anthocyanins that made the film easier to absorb water when RRA content was too high.
330 Hence, the results indicated that addition of a relatively low content of RRA in the GGG
331 film beneficially lowered its mainly consequently reducing the water evaporation of
332 packaged foods.

333 The GGG film had an oxygen permeability (OP) of $10.05 \text{ cm}^3 \cdot \mu\text{m} \cdot \text{m}^{-2} \cdot \text{d}^{-1} \cdot \text{kPa}^{-1}$ (Fig. 3D),
334 which was much lower than low density polyethylene (LDPE) ($1900 \text{ cm}^3 \cdot \mu\text{m} \cdot \text{m}^{-2} \cdot \text{d}^{-1} \cdot \text{kPa}^{-1}$)
335 ¹) and higher than poly(vinylidene chloride) (PVDC) ($0.1\text{--}3 \text{ cm}^3 \cdot \mu\text{m} \cdot \text{m}^{-2} \cdot \text{d}^{-1} \cdot \text{kPa}^{-1}$) and
336 ethylene-vinyl alcohol copolymers (EVOH) ($0.77 \text{ cm}^3 \cdot \mu\text{m} \cdot \text{m}^{-2} \cdot \text{d}^{-1} \cdot \text{kPa}^{-1}$), but comparable
337 to polyvinyl chloride (PVC) ($20\text{--}80 \text{ cm}^3 \cdot \mu\text{m} \cdot \text{m}^{-2} \cdot \text{d}^{-1} \cdot \text{kPa}^{-1}$)⁴⁹. The increase of RRA content,
338 caused the OP value of GGG-RRA films to slightly decrease to $6.33 \times 10^{-2} \text{ cm}^3 \cdot \mu\text{m} \cdot \text{m}^{-2} \cdot \text{d}^{-1} \cdot \text{kPa}^{-1}$
339 ¹ (GGG-RRA20 film). The OP of the films was closely related to the diffusion path
340 of oxygen within the film. The decrease of OP resulting from the increase in RRA content
341 could be due to that the stronger crosslinking of gelatin and gellan gum leading to a
342 reduction of the free volume for oxygen to pass through the films. The low OP of the GGG-
343 RRA films may reduce the oxidation content of packaged foods.

344 **3.4. Electrochemical writing on GGG-RRA film.** In order to write information on the
345 films using the electrochemical method, a hydrogel needed to be firstly fabricated. In this
346 study, a firm gel with a good toughness was facilely formed after the GGG-RRA solution
347 was cooled down without further treatment (Fig. 4A), attributed to the good gelation ability
348 of gelatin and gellan gum. It is well known that the color of anthocyanins is dependent on
349 pH condition⁵⁰, so the principle of electrochemical writing on the hydrogel can be
350 expressed as in scheme 1. When the Pt needle was connected to the anode of the
351 electrochemical workstation, a localized low pH condition was generated in the hydrogel

352 due to the anodic water electrolysis reaction (equation 12) so that anthocyanins turned to
353 acid color (orange red). On the contrary, when the Pt needle was connected to the cathode
354 of the electrochemical workstation, a localized high pH condition was generated in the
355 hydrogel due to the cathodic water electrolysis reaction (equation 13) and therefore
356 anthocyanins turned to basic color (yellow).



359 The movement of the Pt needle along the horizontal plane was controlled by a mechanical
360 arm to produce desired patterns. After being written on the hydrogels, the patterns were
361 preserved by immediately drying the hydrogels to films. Apart from the current direction,
362 the current magnitude could also make the color of the patterns different. When the current
363 increased from 1 to 6 mA, the pattern “1” turned more acid (Fig. 4B) or basic colors (Fig.
364 4C). This was because a greater current led to more intense water electrolysis reaction and
365 thus a greater acid or basic condition. Accordingly, multicolor patterns could be written on
366 one film by tuning the current direction and magnitude. As shown in Fig. 4D and 4E, the
367 flower with orange red petals and green calyces, and the apple with orange red fruit and
368 yellow leaves were respectively drawn on individual films.

369 **3.5. Color stability and gas sensing ability.** The self-stability of the films and the
370 written patterns are of great importance for the practical application of the films. Fig. 5A
371 shows the images of the GGG-RRA10 film with red and yellow patterns stored at 75% for
372 30 d at 4, 25 and 37 °C. The color of the film and patterns gradually faded during storage.
373 Especially at a higher temperature (37 °C), the film obviously turned less red and the

374 patterns seriously discolored after 30 d. To describe the degree of discoloration, the relative
375 color change (S) of the film and patterns was tested and shown in Fig. 5B. The S values of
376 films and patterns increased slightly overall. In contrast, the S values were higher at a
377 higher temperature for both the film and the patterns. At a certain temperature, the S values
378 of the yellow pattern were higher than that of the red pattern followed by the film,
379 indicating that the film had greater color stability than the red pattern and then the yellow
380 pattern. Generally, the anthocyanins were more stable at lower pH.⁵¹ The reason why the
381 red pattern was less stable than the film remained unclear.

382 Before the film was employed as a gas sensor in the packaging system, its sensing ability
383 to acid and basic gas were investigated. As shown in Fig. 5C and 5D, the GGG-RRA film
384 gradually turned to redder after exposure to acetic acid gas, and turned to green after
385 exposed to ammonia gas. This result suggested that the GGG-RRA film could be used to
386 indicate the food spoilage when either acid or basic gases were the dominant volatile gases.
387 As for the written patterns on the film, the red triangle maintained its original color in
388 response to acetic acid (Fig. 5C) but gradually faded in response to ammonia (Fig. 6D). At
389 the same time, the yellow triangle maintained yellow in response to ammonia (Fig. 6D)
390 while gradually fading in response to acetic acid (Fig. 6C). Hence, to save the written
391 information on the film, the films with red color patterns and yellow patterns could be used
392 to indicate food spoilage during which acid gases and basic were the main volatile gases,
393 respectively.

394 **3.6. Application of films for indicating milk and fish spoilage.** In this study, the GGG-
395 RRA10 film was selected to indicate food quality, considering the effect of the
396 anthocyanins concentration on the color visibility and gas sensitivity of the films discussed

397 in our previous study.¹² The GGG-RRA10 films with red pattern “F” and yellow pattern
398 “F” were used to monitor milk and fish spoilage, respectively. As shown in Fig. S1, the
399 films were fixed on the lid to cover the hole that worked as the detection window through
400 which the volatile gases generated from milk and fish diffused to contact with the film and
401 make a color change of the film. In this way, the water vapor inside of the dishes could
402 permeate through the film to the external environment to reduce the film swelling that
403 might cause anthocyanins to leach from the film.

404 Fig. 6A shows the color change of the GGG-RRA10 film during the milk spoilage. With
405 the increase of time, the film turned to be redder. The color change could also be seen from
406 the color parameters, namely red (R), green (G) and blue (B). As shown in Fig. 6B, the R
407 value increased from 232 to 253, indicating a deeper red color, while G and B value did
408 not significantly change. The color change of the film implied that acid volatile gases were
409 generated during the milk spoilage. Similar phenomena were also observed in a previous
410 study.¹³ This was largely due to the generation of organic acids during anaerobic respiration
411 of anaerobic bacteria or facultative anaerobic bacteria under hypoxic or anaerobic
412 condition. It is worth mentioning that the low OP of GGG-RRA10 film might contribute
413 to a hypoxic condition for the anaerobic respiration of spoilage bacteria. The acidity of the
414 milk was an important index to evaluate the freshness of milk. A higher acidity value
415 indicated a larger amount of acid components and therefore an inferior freshness. As shown
416 in Fig. 6B, the acidity of the milk increased from 14.78 to 25.67 °T after a 48 h storage at
417 25 °C. According to Chinese standard (GB 19645-2010), the acidity value of pasteurized
418 milk should be under 18 °T to ensure quality. In this study, the acidity of the reached to

419 18 °T at nearly 25 h, while at this point the R value of the film was nearly 240. This implied
420 that if the R value of the film was higher than 240, the milk sample should not be consumed.

421 Fig. 6C shows the color change of the GGG-RRA10 film during the spoilage of black
422 carp. The film gradually turned from initial orange red to green (4 d) and then yellow green
423 (8 d). Accordingly, the color parameter R decreased, and G increased from 0 d to the 4 d
424 (Fig. 6D). However, the R and G value did not dramatically change after 4 d. Meanwhile,
425 the B value decreased over time from initial an 144 to final 18, indicating a deeper yellow
426 color (the complementary color of blue). Hence, the B value could be used as a
427 characteristic parameter for the color change of the film. The color change of the film could
428 be mainly induced by the volatile basic gases, such as ammonia, trimethylamine and
429 dimethylamine, generated from the black carp. Fig. 6D shows the TVB-N content of the
430 black carp. It rose from 4.74 mg/100g at 0 d to 53.71 mg/100g at 9 d at 4 °C. The generation
431 of TVB-N was due to the decomposition of proteins by bacteria and enzymes. According
432 to Chinese Standard (GB 2733-2015), the rejection limit of TVB-N level for black carp is
433 20 mg/100 g. In this study, the TVB-N value rose to 20 mg/100 g at nearly 5.5 d, when the
434 B value of the film was around 87. This implied that if the B value of the film was lower
435 than 87, then the fish sample should not be consumed.

436 For the written patterns “F” on the GGG-RRA10 films that were used for either milk or
437 fish spoilage, as expect, they retained a clear color and shape (Fig. 6A and 6C). As can be
438 seen from the Fig. S2A, R, G, and B values of the red “F” did not obviously change,
439 indicating a good color stability. Although the B value of the yellow “F” significantly
440 decreased (Fig. S2B), the pattern “F” still kept a bright yellow color because of the weak

441 fluctuation of R and G values. Hence, the GGG-RRA film combined with written pattern
442 could be used to indicate the milk and fish spoilage.

443 As mentioned above, when the GGG-RRA-10 film was used to indicate the milk and
444 fish spoilage, the film showed visible color changes while the written patterns on the film
445 maintained good shapes and colors. As the GGG-RRA films were made from degradable
446 and edible biomaterials, and the patterns were in situ drawn on the films by using
447 electrochemical method without the need of inks, they should have a great potential for
448 practical application in intelligent food packaging.

449 **ACKNOWLEDGMENT**

450 The authors gratefully acknowledge the financial support provided by the Postgraduate
451 Research & Practice Innovation Program of Jiangsu Province (KYCX17_1798), the
452 National Science and Technology Support Program (2015BAD17B04), the National Key
453 Research and Development Program of China (2016YFD0401104), the National Natural
454 Science Foundation of China (31671844, 31601543), China Postdoctoral Science
455 Foundation (2013M540422, 2014T70483, 2016M590422), the Natural Science
456 Foundation of Jiangsu Province (BK20160506, BE2016306), International Science and
457 Technology Cooperation Project of Jiangsu Province (BZ2016013), Suzhou Science and
458 Technology Project (SNG201503) and Priority Academic Program Development of
459 Jiangsu Higher Education Institutions (PAPD). We also would like to thank our colleagues
460 in School of Food and Biological Engineering who provided assistance in this study.

461 **NOTES**

462 The authors declare no competing financial interest.

463 **Supporting Information description**

464 There were two figures in the supporting information file. Fig. S1 the photo of the
465 device that was used to detect milk and fish spoilage. Fig. S2 was the change of the R,
466 G, and B values of written patterns “F” on the GGG-RRA10 film used to monitor milk
467 and fish spoilage.

468

469 **REFERENCES**

- 470 1. Realini, C. E.; Marcos, B., Active and intelligent packaging systems for a modern society.
471 *Meat Sci.* **2014**, *98*, 404-19.
- 472 2. Ghaani, M.; Cozzolino, C. A.; Castelli, G.; Farris, S., An overview of the intelligent
473 packaging technologies in the food sector. *Trends Food Sci. Technol.* **2016**, *51*, 1-11.
- 474 3. Pacquit, A.; Frisby, J.; Diamond, D.; Lau, K.; Farrell, A.; Quilty, B.; Diamond, D.,
475 Development of a smart packaging for the monitoring of fish spoilage. *Food Chem.* **2007**, *102*,
476 466-470.
- 477 4. Rukchon, C.; Nopwinyuwong, A.; Trevanich, S.; Jinkarn, T.; Suppakul, P., Development of
478 a food spoilage indicator for monitoring freshness of skinless chicken breast. *Talanta* **2014**, *130*,
479 547-54.
- 480 5. Dainelli, D.; Gontard, N.; Spyropoulos, D.; Zondervan-van den Beuken, E.; Tobback, P.,
481 Active and intelligent food packaging: legal aspects and safety concerns. *Trends Food Sci.*
482 *Technol.* **2008**, *19*, S103-S112.
- 483 6. Zhang, X.; Lu, S.; Chen, X., A visual pH sensing film using natural dyes from *Bauhinia*
484 *blakeana* Dunn. *Sensors Actuators B: Chem.* **2014**, *198*, 268-273.
- 485 7. Luchese, C. L.; Abdalla, V. F.; Spada, J. C.; Tessaro, I. C., Evaluation of blueberry residue
486 incorporated cassava starch film as pH indicator in different simulants and foodstuffs. *Food*
487 *Hydrocoll.* **2018**, *82*, 209-218.
- 488 8. Pereira, V. A.; de Arruda, I. N. Q.; Stefani, R., Active chitosan/PVA films with
489 anthocyanins from *Brassica oleraceae* (Red Cabbage) as Time–Temperature Indicators for
490 application in intelligent food packaging. *Food Hydrocoll.* **2015**, *43*, 180-188.
- 491 9. Saliu, F.; Della Pergola, R., Carbon dioxide colorimetric indicators for food packaging
492 application: Applicability of anthocyanin and poly-lysine mixtures. *Sensors Actuators B: Chem.*
493 **2018**, *258*, 1117-1124.
- 494 10. Silva-Pereira, M. C.; Teixeira, J. A.; Pereira-Júnior, V. A.; Stefani, R., Chitosan/corn starch
495 blend films with extract from *Brassica oleraceae* (red cabbage) as a visual indicator of fish
496 deterioration. *LWT - Food Sci. Technol.* **2015**, *61*, 258-262.
- 497 11. Wei, Y.-C.; Cheng, C.-H.; Ho, Y.-C.; Tsai, M.-L.; Mi, F.-L., Active gellan gum/purple sweet
498 potato composite films capable of monitoring pH variations. *Food Hydrocoll.* **2017**, *69*, 491-502.
- 499 12. Zhai, X.; Shi, J.; Zou, X.; Wang, S.; Jiang, C.; Zhang, J.; Huang, X.; Zhang, W.; Holmes, M.,
500 Novel colorimetric films based on starch/polyvinyl alcohol incorporated with roselle
501 anthocyanins for fish freshness monitoring. *Food Hydrocoll.* **2017**, *69*, 308-317.
- 502 13. Ma, Q.; Wang, L., Preparation of a visual pH-sensing film based on tara gum
503 incorporating cellulose and extracts from grape skins. *Sensors Actuators B: Chem.* **2016**, *235*,
504 401-407.
- 505 14. Ma, Q.; Ren, Y.; Gu, Z.; Wang, L., Developing an intelligent film containing *Vitis*
506 *amurensis* husk extracts: The effects of pH value of the film-forming solution. *J. Clean. Prod.*
507 **2017**, *166*, 851-859.
- 508 15. Kuswandi, B.; Jayus; Larasati, T. S.; Abdullah, A.; Heng, L. Y., Real-Time Monitoring of
509 Shrimp Spoilage Using On-Package Sticker Sensor Based on Natural Dye of Curcumin. *Food Anal.*
510 *Methods* **2011**, *5*, 881-889.
- 511 16. Ma, Q.; Du, L.; Wang, L., Tara gum/polyvinyl alcohol-based colorimetric NH₃ indicator
512 films incorporating curcumin for intelligent packaging. *Sensors Actuators B: Chem.* **2017**, *244*,
513 759-766.

- 514 17. Liu, J.; Wang, H.; Wang, P.; Guo, M.; Jiang, S.; Li, X.; Jiang, S., Films based on κ-
515 carrageenan incorporated with curcumin for freshness monitoring. *Food Hydrocoll.* **2018**.
- 516 18. Musso, Y. S.; Salgado, P. R.; Mauri, A. N., Smart edible films based on gelatin and
517 curcumin. *Food Hydrocoll.* **2017**, *66*, 8-15.
- 518 19. Otsuki, T.; Matsufuji, H.; Takeda, M.; Toyoda, M.; Goda, Y., Acylated anthocyanins from
519 red radish (*Raphanus sativus* L.). *Phytochemistry* **2002**, *60*, 79-87.
- 520 20. Matsufuji, H.; Kido, H.; Misawa, H.; Yaguchi, J.; Otsuki, T.; Chino, M.; Takeda, M.;
521 Yamagata, K., Stability to Light, Heat, and Hydrogen Peroxide at Different pH Values and DPPH
522 Radical Scavenging Activity of Acylated Anthocyanins from Red Radish Extract. *J. Agric. Food.*
523 *Chem.* **2007**, *55*, 3692-3701.
- 524 21. Park, N. I.; Xu, H.; Li, X.; Jang, I. H.; Park, S.; Ahn, G. H.; Lim, Y. P.; Kim, S. J.; Park, S. U.,
525 Anthocyanin Accumulation and Expression of Anthocyanin Biosynthetic Genes in Radish
526 (*Raphanus sativus*). *J. Agric. Food. Chem.* **2011**, *59*, 6034-6039.
- 527 22. Martucci, J. F.; Accareddu, A. E. M.; Ruseckaite, R. A., Preparation and characterization
528 of plasticized gelatin films cross-linked with low concentrations of Glutaraldehyde. *J. Mater. Sci.*
529 **2012**, *47*, 3282-3292.
- 530 23. Guo, J.; Ge, L.; Li, X.; Mu, C.; Li, D., Periodate oxidation of xanthan gum and its
531 crosslinking effects on gelatin-based edible films. *Food Hydrocoll.* **2014**, *39*, 243-250.
- 532 24. Boateng, J.; Burgos-Amador, R.; Okeke, O.; Pawar, H., Composite alginate and gelatin
533 based bio-polymeric wafers containing silver sulfadiazine for wound healing. *Int. J. Biol.*
534 *Macromol.* **2015**, *79*, 63-71.
- 535 25. Samp, M. A.; Iovanac, N. C.; Nolte, A. J., Sodium Alginate Toughening of Gelatin
536 Hydrogels. *ACS Biomater. Sci. Eng.* **2017**, *3*.
- 537 26. Qiao, C.; Ma, X.; Zhang, J.; Yao, J., Molecular interactions in gelatin/chitosan composite
538 films. *Food Chem.* **2017**, *235*, 45-50.
- 539 27. Zia, K. M.; Tabasum, S.; Khan, M. F.; Akram, N.; Akhter, N.; Noreen, A.; Zuber, M., Recent
540 trends on gellan gum blends with natural and synthetic polymers: A review. *Int. J. Biol.*
541 *Macromol.* **2018**, *109*, 1068-1087.
- 542 28. Ferris, C. J.; Gilmore, K. J.; Wallace, G. G.; Panhuis, M. I. H., Modified gellan gum
543 hydrogels for tissue engineering applications. *Soft Matter* **2013**, *9*, 3705-3711.
- 544 29. Lee, K. Y.; Shim, J.; Lee, H. G., Mechanical properties of gellan and gelatin composite
545 films. *Carbohydr. Polym.* **2004**, *56*, 251-254.
- 546 30. Xu, X.-J.; Fang, S.; Li, Y.-H.; Zhang, F.; Shao, Z.-P.; Zeng, Y.-T.; Chen, J.; Meng, Y.-C., Effects
547 of low acyl and high acyl gellan gum on the thermal stability of purple sweet potato
548 anthocyanins in the presence of ascorbic acid. *Food Hydrocoll.* **2018**.
- 549 31. Robert, T., "Green ink in all colors"—Printing ink from renewable resources. *Prog. Org.*
550 *Coat.* **2015**, *78*, 287-292.
- 551 32. Aznar, M.; Domeño, C.; Nerín, C.; Bosetti, O., Set-off of non volatile compounds from
552 printing inks in food packaging materials and the role of lacquers to avoid migration. *Dyes and*
553 *Pigments* **2015**, *114*, 85-92.
- 554 33. Wang, H.; Qian, J.; Li, H.; Ding, F., Rheological characterization and simulation of
555 chitosan-TiO₂ edible ink for screen-printing. *Prog. Org. Coat.* **2018**, *120*, 19-27.
- 556 34. Wu, S.; Wang, W.; Yan, K.; Ding, F.; Shi, X.; Deng, H.; Du, Y., Electrochemical writing on
557 edible polysaccharide films for intelligent food packaging. *Carbohydr. Polym.* **2018**, *186*, 236-
558 242.
- 559 35. Wang, Z.; Li, Y.; Chen, L.; Xin, X.; Yuan, Q., A study of controlled uptake and release of
560 anthocyanins by oxidized starch microgels. *J. Agric. Food. Chem.* **2013**, *61*, 5880-7.

- 561 36. Xiaowei, H.; Xiaobo, Z.; Jiewen, Z.; Jiyong, S.; Zhihua, L.; Tingting, S., Monitoring the
562 biogenic amines in Chinese traditional salted pork in jelly (Yao-meat) by colorimetric sensor
563 array based on nine natural pigments. *Int. J. Food Sci. Tech.* **2015**, *50*, 203-209.
- 564 37. Lixin, L.; Weizhou, Z.; Zhiye, L.; Yali, T., Development and Application of Time-
565 temperature Indicators Used on Food during the Cold Chain Logistics. *Packag. Technol. Sci.*
566 **2013**, *26*, 80-90.
- 567 38. Cai, J.; Chen, Q.; Wan, X.; Zhao, J., Determination of total volatile basic nitrogen (TVB-N)
568 content and Warner-Bratzler shear force (WBSF) in pork using Fourier transform near infrared
569 (FT-NIR) spectroscopy. *Food Chem.* **2011**, *126*, 1354-1360.
- 570 39. Choi, I.; Lee, J. Y.; Lacroix, M.; Han, J., Intelligent pH indicator film composed of
571 agar/potato starch and anthocyanin extracts from purple sweet potato. *Food Chem.* **2017**, *218*,
572 122-128.
- 573 40. Pranoto, Y.; Lee, C. M.; Park, H. J., Characterizations of fish gelatin films added with
574 gellan and κ -carrageenan. *LWT - Food Sci. Technol.* **2007**, *40*, 766-774.
- 575 41. Fonkwe, L. G.; Narsimhan, G.; Cha, A. S., Characterization of gelation time and texture of
576 gelatin and gelatin-polysaccharide mixed gels. *Food Hydrocoll.* **2003**, *17*, 871-883.
- 577 42. Jin, W.; Shih - Chien, C.; M., P. E.; K., K. T., Effects of phenolic compounds on gelation
578 behavior of gelatin gels. *J. Polym. Sci., Part A: Polym. Chem.* **2001**, *39*, 224-231.
- 579 43. Picone, C. S. F.; Cunha, R. L., Influence of pH on formation and properties of gellan gels.
580 *Carbohydr. Polym.* **2011**, *84*, 662-668.
- 581 44. Jiang, Y.; Li, Y.; Zhi, C.; Leng, X., Study of the Physical Properties of Whey Protein Isolate
582 and Gelatin Composite Films. *J. Agric. Food. Chem.* **2010**, *58*, 5100-5108.
- 583 45. Bitencourt, C. M.; Fávoro-Trindade, C. S.; Sobral, P. J. A.; Carvalho, R. A., Gelatin-based
584 films additivated with curcuma ethanol extract: Antioxidant activity and physical properties of
585 films. *Food Hydrocoll.* **2014**, *40*, 145-152.
- 586 46. Prodpran, T.; Benjakul, S.; Phatcharat, S., Effect of phenolic compounds on protein
587 cross-linking and properties of film from fish myofibrillar protein. *Int. J. Biol. Macromol.* **2012**,
588 *51*, 774-782.
- 589 47. Parris, N.; Coffin, D. R.; RF, J.; H, P., Composition factors affecting the water vapor
590 permeability and tensile properties of hydrophilic films. *J. Agric. Food Chem.* **1997**, *45*, 1596-
591 1599.
- 592 48. Jakobek, L., Interactions of polyphenols with carbohydrates, lipids and proteins. *Food*
593 *Chem.* **2015**, *175*, 556-567.
- 594 49. Garusinghe, U. M.; Varanasi, S.; Raghuvanshi, V. S.; Garnier, G.; Batchelor, W.,
595 Nanocellulose-montmorillonite composites of low water vapour permeability. *Colloids Surf.*
596 *Physicochem. Eng. Aspects* **2018**, *540*, 233-241.
- 597 50. Castañeda-Ovando, A.; Pacheco-Hernández, M. d. L.; Páez-Hernández, M. E.; Rodríguez,
598 J. A.; Galán-Vidal, C. A., Chemical studies of anthocyanins: A review. *Food Chem.* **2009**, *113*, 859-
599 871.
- 600 51. Torskangerpoll, K.; Andersen, O. M., Colour stability of anthocyanins in aqueous
601 solutions at various pH values. *Food Chem.* **2005**, *89*, 427-440.

602

603 **Figure captions**

604 **Fig. 1.** The color (A) and UV-vis spectra (B) of RRA anthocyanins extract solution at pH 2-12, and
605 the color (C) and UV-vis spectra (D) of GGG-RRA10 film at pH 2-12. Insets of (B) and (D) were
606 the change of A_{580}/A_{510} of the RRA solution and GGG-RRA10 film with the change of pH,
607 respectively.

608 **Fig. 2.** The SEM images of cross sections of GGG (A), GGG-RRA5 (B), GGG-RRA10 (C), GGG-
609 RRA15 (D) and GGG-RRA20 film (E).

610 **Fig. 3.** The mechanical properties (A), transparencies (B), WVP (C) and OP (D) of the GGG and
611 GGG-RRA films.

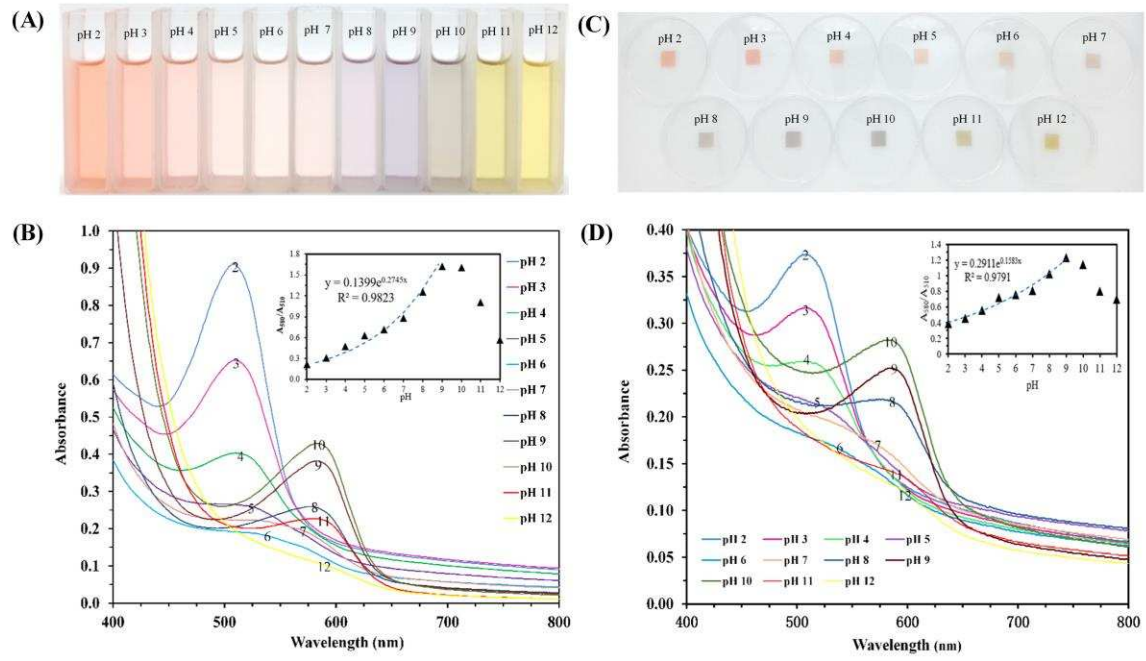
612 **Scheme 1.** The principle of electrochemical writing on GGG-RRA film.

613 **Fig. 4.** The photo of GGG-RRA10 hydrogel (A); the images of pattern “1” at different current
614 magnitude when the Pt needle was connected with the anode (B) and cathode (C) of the
615 electrochemical workstation; the images of multicolor pattern flower (D) and apple (E) written on
616 the film.

617 **Fig. 5.** Images (A) and the corresponding S values (B) of the GGG-RRA10 film with written patterns
618 stored at 4, 25 and 37 °C for 30 days; the color response of the GGG-RRA10 film with written
619 patterns towards acetic acid (C) and ammonia gas (D).

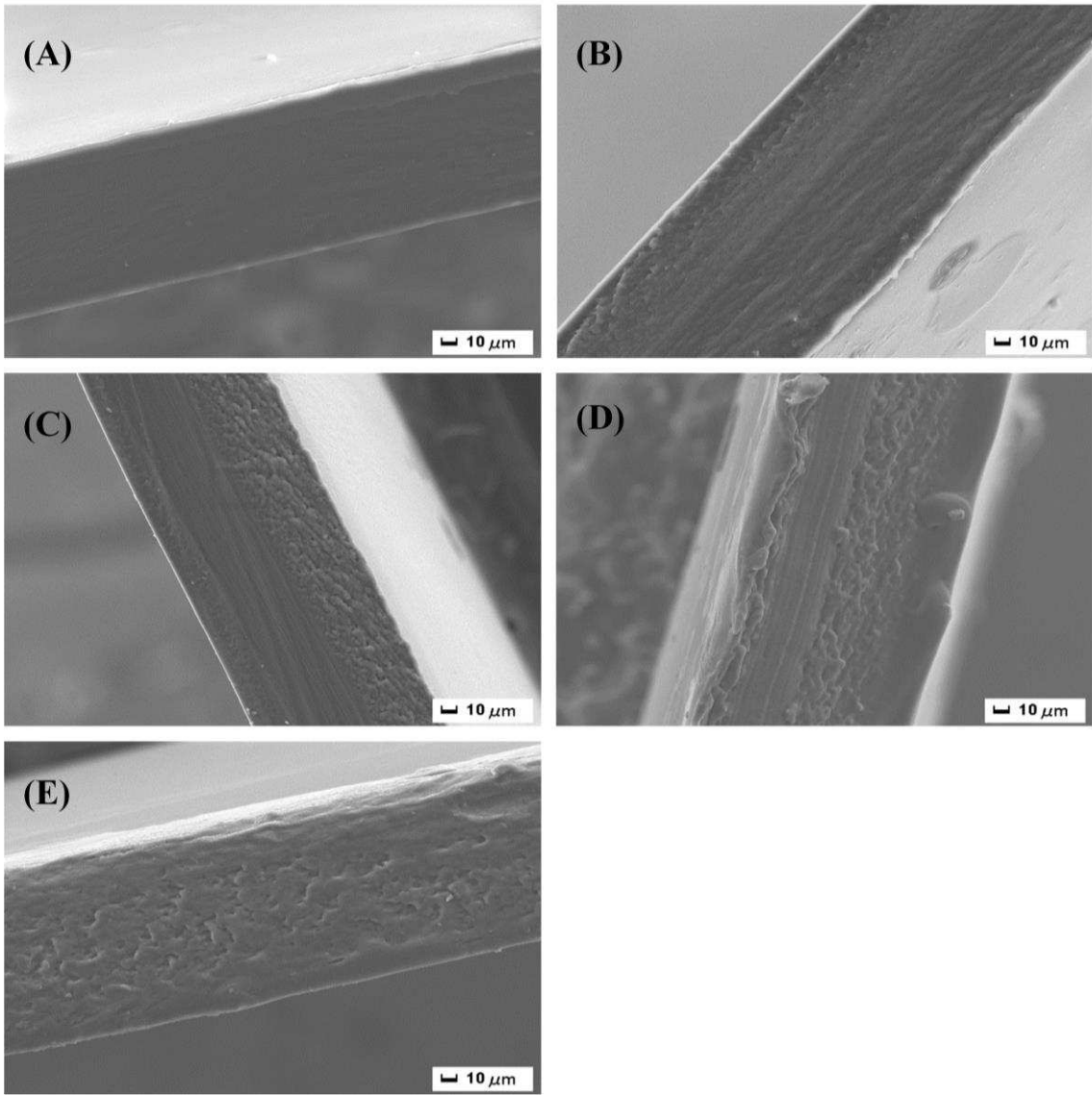
620 **Fig. 6.** Images of GGG-RRA10 film with red pattern “F” when used to monitor the milk spoilage
621 at 25 °C (A), and the corresponding R, G, B values changes of the film and the acidity change of
622 the milk (B); Images of GGG-RRA10 film with yellow pattern “F” when used to monitor the black
623 carp spoilage at 4 °C (C), and the corresponding R, G, B value changes of the film and the TVB-N
624 content changes of the black carp (D).

625 Figure 1.



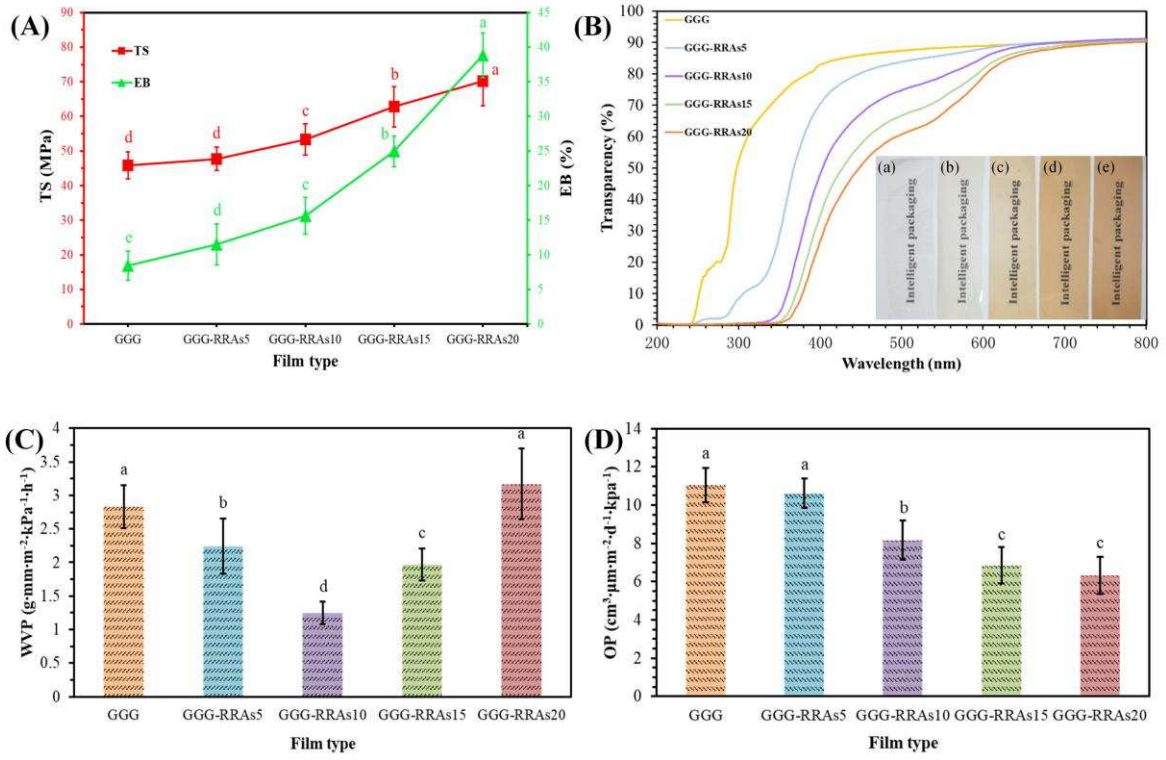
626

627 Figure 2.



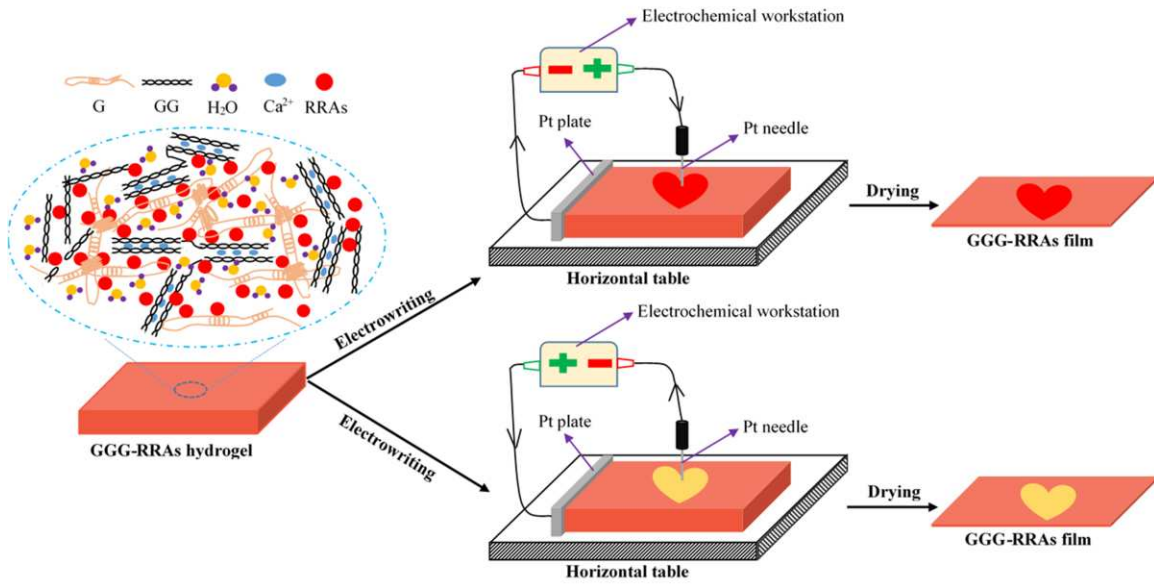
628

629 Figure 3.

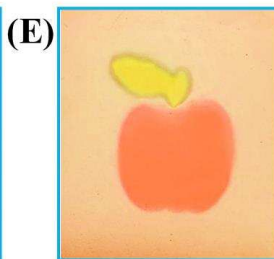
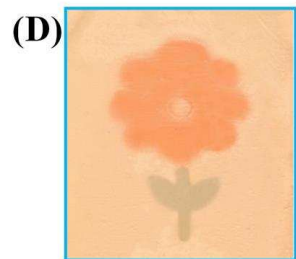
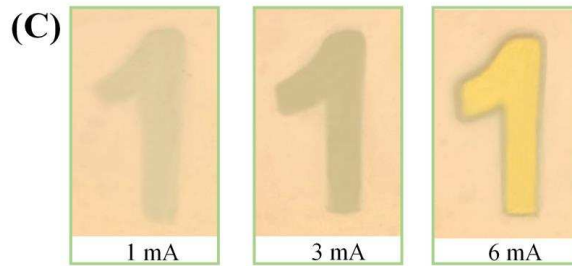
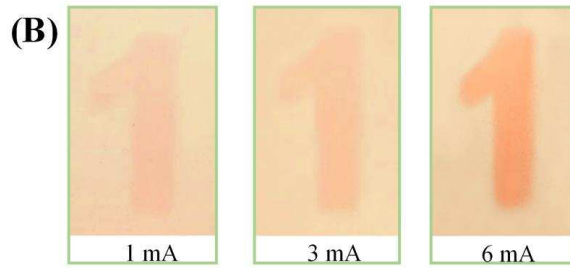
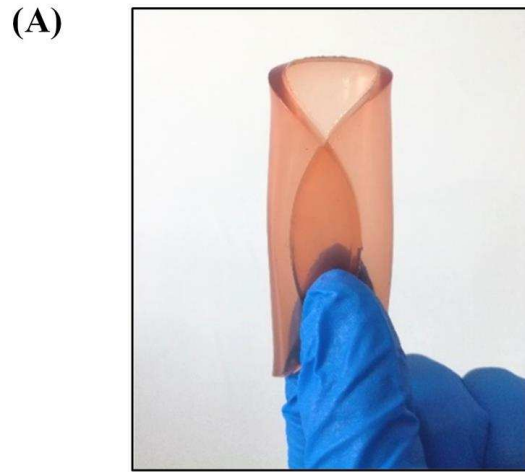


630

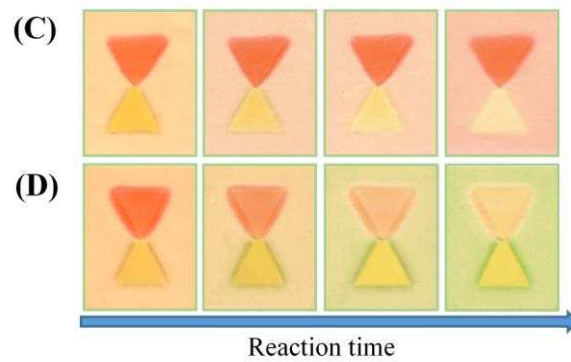
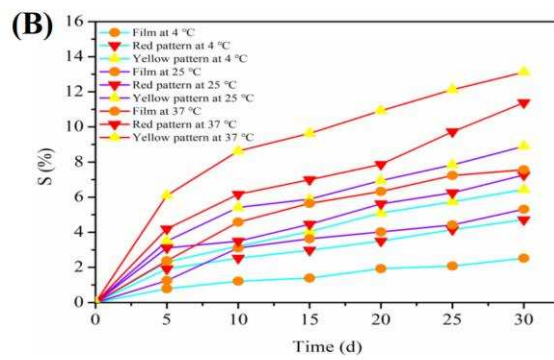
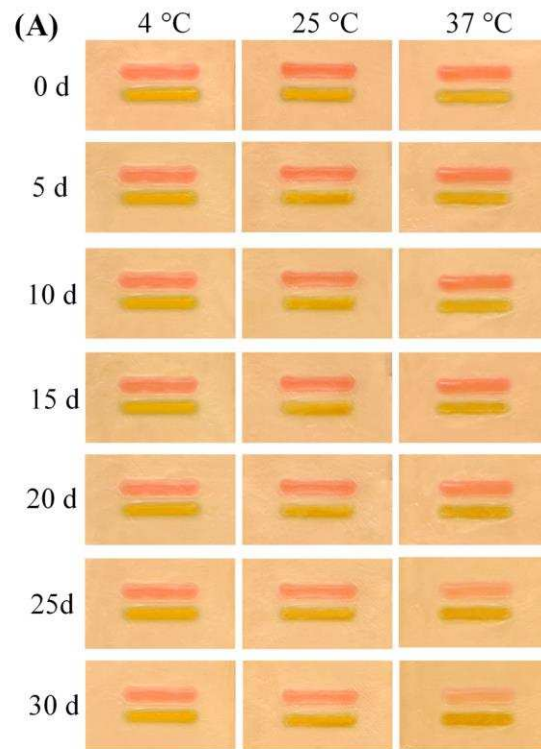
631 Scheme 1.



632

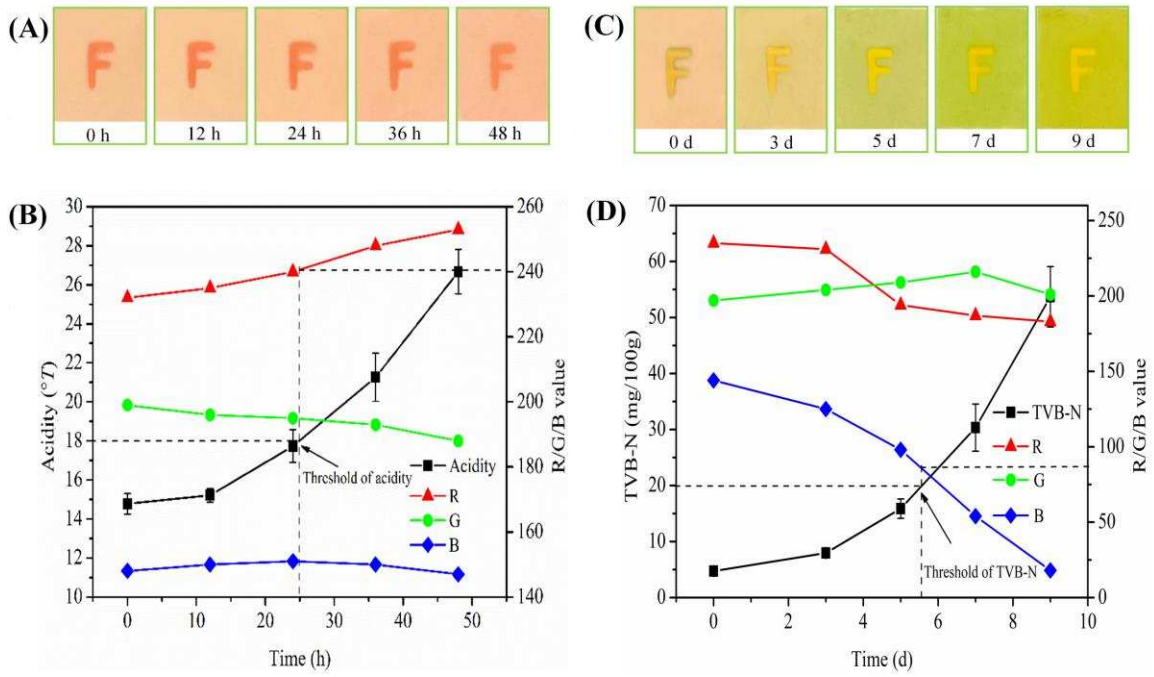


635 Figure 5.



636

637 Figure 6.



638